SURE 静岡大学学術リポジトリ
Shizuoka University REpository

Comparative study on a novel lobule structure of the zebrafish liver and that of the mammalian liver

メタデータ	言語: English 出版者: Springer Nature 公開日: 2022-04-05 キーワード (Ja): キーワード (En): liver lobule, bile duct, portal triad, teleost, evolution 作成者: Ota, Noriaki, Shiojiri, Nobuyoshi メールアドレス: 所属:
URL	http://hdl.handle.net/10297/00028845

Comparative study on a novel lobule structure of the zebrafish liver and that of the mammalian liver

Noriaki Ota[1] and Nobuyoshi Shiojiri[2]

[1]Graduate School of Science and Technology, Shizuoka University, Oya 836, Suruga-ku, Shizuoka City, Shizuoka 422-8529, Japan.

[2]Department of Biology, Faculty of Science, Shizuoka University, Oya 836, Suruga-ku, Shizuoka City, Shizuoka 422-8529, Japan.

Corresponding author: Nobuyoshi Shiojiri, Department of Biology, Faculty of Science, Shizuoka University, Oya 836, Suruga-ku, Shizuoka City, Shizuoka 422-8529, Japan. Tel.: 81-54-238-4780; Fax: 81-54-238-0986. E-mail: shiojiri.nobuyoshi@shizuoka.ac.jp

Running title: Architecture of zebrafish liver

Electronic word count: 7612 words

Number of figures and tables: 8 figures, 0 tables, 8 supplementary figures, 2 supplementary movies, 5 supplementary tables.

Abstract

The mammalian liver has a lobule structure with a portal triad consisting of the portal vein, hepatic artery and bile duct, which exhibits zonal gene expression, whereas those of teleosts do not have a portal triad. It remains to be demonstrated what kind of the unit structures they have, including their gene expression patterns. The aims of the present study were to demonstrate the unit structure of the teleost liver and discuss it in terms of evolution and adaptation in vertebrates and the use of teleosts as an alternative model for human disease. The zebrafish liver was examined as a representative of teleosts with respect to its morphological architecture and gene expression. A novel, polygonal lobule structure was detected in the zebrafish liver. In it portal veins and central veins were distributed at the periphery and center, respectively. Sinusoids connected both veins. Anxa4-positive preductules were incorporated into the tubular lumen of two rows of hepatocytes in sections. Intrahepatic bile ducts resided randomly in the liver lobule. Zebrafish livers did not have zonal gene expression for metabolic pathways examined. The lobules of the zebrafish liver with preductules located in the tubular lumina of hepatocytes may resemble the oval cell reaction of injured livers of mammals, and might convey bile to the intestine more safely than mammalian livers. The gene expression pattern in liver lobules and our liver lobule model of the zebrafish may be important to discuss data obtained in experiments using this animal as an alternative model for human disease.

(250 words)

43 Keywords: liver lobule, bile duct, portal triad, teleost, evolution.

44

45

46

47

48

49

50

51

52

53 Introduction

54

55 In mammalian livers, the hepatic lobule is the smallest histological unit, a polygonal pillar
56 structure, in which hepatocytes and sinusoidal endothelial cells are radially aligned from the center.
57 The lobule is nourished by a dual vascular system, the hepatic artery from the heart, and the portal
58 vein from the intestinal tract, both of which are located in the periphery of the lobule. Their blood
59 may mix in the periphery of the lobule, after which it passes through sinusoids, is collected in the
60 central vein of the lobule, and then flows out of the liver. In the periphery of the lobule, the portal
61 triad consisting of the portal vein, hepatic artery and intrahepatic bile duct is formed. Bile
62 produced by hepatocytes flows through bile canaliculi, ductules, intrahepatic bile ducts along portal
63 veins, and subsequently through the extrahepatic bile duct to the intestine. In mammalian livers,
64 zonal gene expression in the lobule is established (Moorman et al. 1988; Doi et al. 2007; Gerbal-
65 Chaloin et al. 2014). This leads to efficient metabolism of various substances, including ammonia
66 and glucose (Ohno et al. 2008; Ghafoory et al. 2013).

67 By contrast, we have recently shown that, among vertebrates, the teleost may have evolved
68 a specialized liver architecture with independent configuration of portal veins and intrahepatic bile
69 ducts in contrast to the portal triad found in mammalian livers (Shiojiri et al. 2017; Ota et al. 2021).
70 The ancestral portal triad is detected in the cyclostomes and cartilaginous fishes that may have
71 branched off from the early vertebrates as well as tetrapods (Umezu et al. 2012). Among the ray-
72 finned fish, the early branched species have a portal triad, but this feature is not found in teleosts
73 such as the zebrafish and medaka. In other words, the portal triad is a structural feature that may

74 be conserved from the birth of the liver during vertebrate evolution, and teleosts may have acquired
75 a novel liver architecture that may have evolved from the ancestral one having the portal triad.
76 Although the unit structure of the teleost has been postulated to be a hepatic tubule or hepatic lobule,
77 this has remained controversial (Hampton et al. 1988; Rocha et al. 1994; Petcoff et al. 2006;
78 Hardman et al. 2007; Yao et al. 2012; Faccioli et al. 2014). In addition, little is known about the
79 hepatic zonation in the teleost except for some fish, including the Salmonidae species (Schär et al.
80 1985). Thus, studying the characteristics of newly acquired liver architectures of the teleost from
81 various aspects, including the tubule/lobule structure and zonation, may make a significant
82 contribution to understanding of the evolution and adaptation mechanisms of the ray-finned fish.
83 In recent years, from the viewpoint of research cost, there are many uses of alternative
84 organisms to laboratory animal mammals when conducting research on the treatment or
85 regeneration of human liver, toxicity tests, research on genetic diseases and so on（Lorent et al.
86 2004; Matthews et al. 2004; Cui et al. 2013; Lu et al. 2015). On the other hand, caution should
87 be paid when the zebrafish is used to replace mammals in liver research because the liver structure
88 is different between teleosts and mammals (Shiojiri et al. 2017; Ota et al. 2021). A detailed
89 comparison of the liver architectures of teleosts and mammals, and an accurate model of the liver
90 lobule of teleosts may be important to evaluate the usefulness and limitations of the zebrafish liver
91 as an alternative for mammalian livers.
92 The present study is a detailed histological and gene expression analysis of the zebrafish
93 liver in comparison with the mammalian mouse liver, based on the fact that the teleost liver has a
94 novel structure that may have evolved from a mammalian-type structure. A novel liver lobule

model of the zebrafish is proposed and discussed in terms of the evolution and adaptation of liver structures in vertebrates, and the use of the zebrafish as an alternative model for human liver disease.

Materials and Methods

Animals

Wild-type zebrafish (Line: RIKEN WT) were obtained from the "National BioResource Project, Zebrafish, NBRP/Brain Science Institute, RIKEN", and adult fish 3 to 5 months old (males and females), which were kept at 27°C, were used in the present study. C3H/HeSlc mice 3 to 6 month old (Japan SLC, Hamamatsu, Japan) were also used. All animal experiments were carried out in compliance with the "Guide for Care and Use of Laboratory Animals of Shizuoka University".

Histology and immunohistochemistry

Livers and associated organs, including the extrahepatic bile duct, pancreas and intestine, were fixed in a cold mixture of 95% ethanol and acetic acid (99:1 v/v) overnight. After dehydration, tissues were embedded in paraffin. Dewaxed serial sections were stained with hematoxylin-eosin (H-E), periodic acid-Schiff-hematoxylin (PAS-H) and for alkaline phosphatase (ALP) activity (Umezu et al. 2012).

Dewaxed sections were also incubated overnight at 4°C with the primary antibodies listed in Supplementary Table 1. In the case of immunofluorescence, after thorough washing with PBS, sections were incubated with the secondary antibodies listed in Supplementary Table 2, and 4',6-

diamidine-2'-phenylindole dihydrochloride (DAPI), for 1 hr at room temperature, washed again, and mounted in buffered glycerol containing p-phenylenediamine.

When a peroxidase-labeled secondary antibody was used, endogenous peroxidase activity in dewaxed sections was blocked by treatment with phosphate-buffered saline (PBS) containing 3% H_2O_2 for 10 min before incubation with the primary antibodies. Then, after thorough washing with PBS, sections were incubated with the secondary antibodies listed in Supplementary Table 2 for 1 hr at room temperature. After thorough washing again, the sections were stained with 3,3'-diaminobenzidine (DAB), and followed by hematoxylin.

Three-dimensional (3D) reconstruction of sinusoidal ALP activity staining

Serial sections of zebrafish livers stained for ALP activity (10 or 13 sections) were manually aligned using MIcrosoft® PowerPoint® 2016, and exported as PNG image data. The aligned image data were processed using the "3D viewer" in Fiji, which is an image processing package (Schmid et al. 2010; Schindelin et al. 2012).

RT-PCR

Total RNA was extracted from liver samples using ISOGEN II (Nippon Gene Co.). cDNA was synthesized from the total RNA, and the PCR reaction was conducted according to Akai et al. (2014). The primers used are shown in Supplementary Table 3.

In situ hybridization (ISH)

Liver tissues used for ISH were fixed at 4°C in MEMFA solution (0.1M 3-morpholinopropanesulfonic acid [MOPS], 2.0 mM O,O'-bis(2-aminoethyl)ethyleneglycol-N,N,N',N'-tetraacetic acid [EGTA], 1.0 mM magnesium sulfate, 3.7% formaldehyde) overnight.

After replacing the fixed solution with 30% sucrose solution, the tissues were embedded with Tissue-Tek O.C.T compound (Sakura Finetek Japan Co., Ltd.) in liquid nitrogen.

Sense and antisense digoxigenin-labeled riboprobes for zebrafish mRNAs were directly prepared using a DIG RNA labeling kit (Roche Diagnostics) with T7 and Sp6 RNA polymerases from PCR fragments that were flanked by T7 and Sp6 promoters on each side. In situ hybridization of frozen sections was carried out according to Akai et al. (2014). The probes used are shown in Supplementary Table 4.

Results

1. Anatomical location and morphology of the zebrafish liver

The liver of the adult zebrafish (male and female) surrounded the intestinal tract, which was folded twice in the body cavity (Supplementary Fig. 1a-c). The liver was a parenchymal mass, but divided into three lobes posteriorly (Supplementary Fig. 1b, c). The pancreas, which had no definite shape, was widely distributed between the liver and intestinal tract (Supplementary Fig. 1c), but sometimes invaded the liver along portal veins (Fig. 1a-d; Supplementary Fig. 2a-c).

The zebrafish had a single extrahepatic bile duct that connected with the small intestine, but it branched into several ducts (hepatic ducts) in the extrahepatic region before connecting with intrahepatic bile ducts (Fig. 1a-i). Direct connections between the extrahepatic bile duct and intrahepatic bile ducts were not found in all three lobes, but only the lobe closest to the intestinal tract had a direct connection with the extrahepatic bile duct (data not shown). It sent intrahepatic

158 bile ducts to the other lobes. Although the extrahepatic bile duct and main pancreatic duct directly
159 joining the pancreas and duodenum ran closely near the small intestine, they independently entered
160 the intestinal tract in the zebrafish, which was in contrast to those of humans and mice (Fig. 1a).
161 Portal veins or afferent vessels from the most anterior segment of the intestinal tract entered
162 the liver from multiple sites that were independent of the course of bile ducts (Fig. 2a). This
163 configuration was different from that of mammals, in which a single portal vein branches in the
164 hilum and enters the liver along bile ducts. Histochemical analyses of ALP activity showed that
165 the ALP-positive hepatic artery entered the liver along bile ducts (Supplementary Fig. 3a-d).
166 ALP-positive vessels in the periportal pancreatic tissue invading the liver, which may also be
167 hepatic arteries, joined hepatic sinusoids (Supplementary Fig. 2a-c). Central veins or efferent
168 vessels exited from several places of the liver but joined into a large vein running to the heart. In
169 addition, a blood vessel from the gonad connected with a central vein in the liver (Supplementary
170 Fig. 4a-e). Portal and central veins did not have any ALP activity.
171
172 2. Lobule structure in zebrafish liver
173 2-1. Vasculature
174 Sinusoidal endothelial cells, which were positive in ALP activity staining, directly
175 connected portal veins with central veins in the zebrafish liver as in mammalian livers (Fig. 2b).
176 When portal and central veins were identified in serial sections from their connections with the
177 intestine and heart, polygonal leaflet structures were detected. In these, central and portal veins
178 were located at the center and periphery, respectively (Fig. 3a, b). When serial sections of ALP

179 activity staining were processed to reconstruct three-dimensional images of the sinusoidal
180 orientation using Fiji, sinusoids ran centripetally from several portal veins in their periphery to a
181 central vein in three dimensions (Fig. 3c; Supplementary movies 1 and 2). Tubules of hepatocytes
182 resided between sinusoids. In terms of the vascular and tubule configuration, the polygonal
183 structures may be lobular units of the zebrafish liver. However, the configuration of the hepatic
184 artery in the zebrafish liver was different from that found in mammalian livers. In the zebrafish,
185 the hepatic artery entered the liver along with bile ducts and portal veins. The hepatic artery
186 resided inside and at the periphery of the lobule, which contrasted with its position (only the
187 periphery of the liver lobule) in mammalian livers (Supplementary Figs. 2a-c, 3a-d).

188 2-2. Biliary system

189 In the lobule, intrahepatic bile ducts did not have any correlation to the configuration of
190 portal veins, and frequently resided inside the lobule (Fig. 3a-c). Anxa4-positive
191 preductules/ductules were reticulated in the entire lobule unit, and cholangiocyets of preductules
192 penetrated into the apical sides of hepatocytes having a tubular lumen, which formed 2-cell plates
193 in section (Fig. 4a, b; Supplementary Fig. 5a, b). Anxa4-positive ductule cells also connected
194 preductules across sinusoids. In the ISH data of *anxa4*, its mRNA exhibited the same expression
195 pattern as in anxa4 immunohistochemistry, indicating that these preductules and ductules were not
196 a substructure made in hepatocytes such as a bile canaliculus (Fig. 4c).

197 2-3. Hepatocytes

198 Because glycogen accumulation and gene expression of ammonia- or drug-metabolizing
199 enzymes and cell adhesion molecules show zonal distribution in liver lobules of humans and mice

200 (Jungermann and Thurman 1992; Ghafoory et al. 2013), we investigated whether the zebrafish liver
201 develops similar zonation. RT-PCR data for gene expression of various mammalian hepatic marker
202 genes in the zebrafish liver, including zonation markers, are shown in Supplementary Table 5.
203 The accumulation of PAS-positive glycogen was uniform in livers of the zebrafish (Fig.
204 5a, h). Whereas phosphoenolpyruvate carboxykinase (PEPCK; *Pck1*) is involved in
205 gluconeogenesis and expressed periportally in mammalian livers (Bartels et al. 1989), expression
206 of *pck1*, which is the ortholog of mouse *Pck1* in the zebrafish, was not restricted to the periportal
207 region, but found throughout the liver (Supplementary Fig. 6c).
208 We next examined gene expression of *oat*, *arg1*, *cps1* and *glul* (ortholog of mammalian
209 glutamine synthase), which are the major components of ammonia decomposition and have
210 complementary zonal expression in mammalian livers (Moorman et al. 1988; Kuo et al. 1991; Yu
211 et al. 2003). When their gene expression was examined using RT-PCR, *oat*, *glula* and *glulb* were
212 expressed, but expression of *arg1* and *cps1* could not be confirmed in the zebrafish liver
213 (Supplementary Table 5). On the other hand, expression of another gene *arg2*, which may have
214 the same function as *arg1*, was confirmed. In mammals, Arg2 is not expressed in the liver (Yu et
215 al. 2003). ISH analysis of the zebrafish liver demonstrated that *oat*, *glul* (*glula* and *glulb*) and *arg2*
216 were uniformly expressed in the whole hepatic lobule (Fig. 5i, Supplementary Fig. 6a, b, d),
217 although in mouse livers GS and Oat were expressed in pericentral hepatocytes (Fig. 5b), and Arg1
218 was expressed in non-pericentral regions (Yu et al. 2003).
219 In mammalian livers, drug-metabolizing enzymes, including Cyp1a2 and Cyp2e1, show
220 zonal expression (Gerbal-Chaloin et al. 2014). In the zebrafish liver, we analyzed the expression

221 of their orthologues *cyp1a* and *cyp2y3*. Expression of both genes was confirmed by RT-PCR
222 (Supplementary Table 5). ISH analyses indicated that *cyp1a* and *cyp2y3* were expressed in the
223 whole liver of the zebrafish whereas both enzyme proteins were restricted to pericentral regions in
224 mice (Fig. 5c, d, j, k).

225 In mammalian livers, E-cadherin and N-cadherin show a zonal expression (Doi et al. 2007;
226 Hempel et al. 2015). In the mouse livers, E-cadherin was expressed in hepatocytes around portal
227 veins but not in hepatocytes around central veins. In contrast, N-cadherin was expressed throughout
228 but upregulated toward hepatocytes around central veins (Fig. 5e-g). In the zebrafish liver, when
229 expression analysis of *cdh1* (*E-cadherin*) and *cdh2* (*N-cadherin*) was performed using RT-PCR,
230 expression of both genes was confirmed (Supplementary Table 5). Next, when their localization
231 was examined with ISH, *cdh1* was found to be expressed in bile duct epithelial cells and ductules,
232 but not in hepatocytes in any region of the liver lobule (Fig. 5l; Supplementary Fig. 7a-c). On the
233 other hand, *cdh2* was strongly expressed in hepatocytes of the whole liver (Fig. 5m; Supplementary
234 Fig. 7d-f). In the zebrafish hepatic lobule, *cdh1* and *cdh2* did not show any zonal expression.

235

236 3. Gene expression in extrahepatic and intrahepatic bile duct system

237 In mammalian livers, gene expression differs in each compartment of the biliary duct
238 system; i.e., the preductules/ductules, intrahepatic bile ducts and extrahepatic bile ducts (Sumazaki
239 et al., 2004; Igarashi et al., 2012). Gene expression in the bile duct system of the zebrafish was
240 examined with RT-PCR and ISH for genes whose expression was confirmed in bile ducts of mice.
241 Although *spp1* and *cftr* were not detected, *epcam*, *hnf1ba*, *hnf1bb* and *slc4a2b* were found to be

242 expressed in RT-PCR analyses of the zebrafish liver (Supplementary Table 5). When their
243 expression was next examined with ISH, *anxa4*, *cdh1*, and *epcam* were found to be expressed in
244 all epithelial cells of preductules/ductules, intrahepatic bile ducts, and the extrahepatic bile duct
245 (Fig. 6a-f). Genes whose expression was confirmed in epithelial cells of intrahepatic and
246 extrahepatic bile ducts but not in preductules/ductules were *slc4a2b*, *hnf1ba* and *hnf1bb* (Fig. 6g-
247 l). *pdx1* was expressed only in extrahepatic bile duct cells (Fig. 6m-o). Genes whose expression
248 was restricted only to preductules/ductules or epithelial cells of intrahepatic bile ducts were not
249 identified in the zebrafish liver (Fig. 7).
250
251 4. Comparison of gene expression between portal veins and central veins
252 In mouse and chicken livers, it has been demonstrated that the expression of several genes,
253 including *Jag1* and *Gja5*, differs between endothelia of portal veins and central veins, and their
254 supporting connective tissues (Jones et al. 2000; Shiojiri et al. 2006). We investigated how the
255 portal vein-specific genes in mouse and chicken livers were expressed in the vasculature of the
256 zebrafish liver. The portal vein-specific expression pattern was not observed for their orthologs
257 *jag1a*, *jag1b*, *gja5a*, and *gja5b* (Fig. 8a-d).
258
259 Discussion
260
261 1. Novel lobule structure in zebrafish liver and evolution

Several reports have shown that a typical lobule structure like that of mammals is not observed in the liver of the teleost, which is often explained as having a “hepatic tubule” as an alternative to the mammalian “hepatic lobule” (Hampton et al. 1988; Rocha et al. 1994; Petcoff et al. 2006; Faccioli et al. 2014). On the other hand, in the medaka liver, the hepatobiliary architecture is based on a polyhedral (hexagonal) structural motif, and parenchymal architecture is more related to that of the mammalian liver than previously believed (Hardman et al. 2007). Yao et al. (2012) has indicated that the hepatic tubules or cords and sinusoids distribute radially around a central vein in the zebrafish liver. In the present study, from detailed three-dimensional analyses of the vascular configuration, including the exact positions of the portal and central veins, we found for the first time that the zebrafish liver had lobules with polygonal structures, in which central veins and portal veins were located at the center and periphery of the lobule, respectively (Fig. 8). Sinusoids connected both veins. Although the lobule found in the zebrafish liver may be conserved in terms of the vascular architecture of the porto-sinusoid-central axis during vertebrate evolution, it had several differences from that of mammals (Fig. 8). These differences may be traits or advantages acquired by teleosts over mammalian-type liver architectures.

The first difference is found in its hepatobiliary system in the lobule (Fig. 8). In mammalian livers, bile produced by hepatocytes flows through bile canaliculi across the hepatic lobule to ductules, and then to intrahepatic bile ducts around portal veins. Mammalian hepatocytes form 1-cell plate. On the other hand, in the zebrafish, intrahepatic bile ducts were not confined to periportal regions, and appeared to be randomly distributed in the liver lobule. Instead of a bile canalicular network in the mammalian liver lobule, the zebrafish liver lobule formed a network of

283 preductules, which resided on the apical membrane of hepatocytes forming a tubular (canalicular)
284 lumen, and ductules. Hepatocytes formed 2-cell plates in sections in the zebrafish. These data
285 indicated that the major pathway for bile transportation across the hepatic lobule was bile canaliculi
286 in mammals, but tubules/preductules and ductules with bile canaliculi in the zebrafish or teleosts.
287 It is known that when the mammalian liver is damaged by some chemical toxins, the adhesion
288 between hepatocytes is weakened, and the bile canaliculus does not normally function, which
289 causes bile to leak out (Kamimoto et al. 2020). Under such conditions, ductule cells around portal
290 veins proliferate and infiltrate into the liver parenchyma, thereby transporting bile compensatorily
291 (Kamimoto et al. 2020). The bile transport system of preductules and ductules in the liver lobule
292 of the zebrafish may be related to this infiltration of ductule cells in liver injury of mammals. The
293 bile might be transported more safely in the zebrafish or teleost livers with well-developed
294 preductules/ductules than in other vertebrates having a mammalian-type bile transport system.

295 Two-hepatocyte cell plates in the zebrafish liver may resemble those of amphibians and
296 birds, although preductules are not detectable in the latter (Shiojiri et al. 2017). Two-hepatocyte
297 cell plates have been shown in fetal human livers (Elias 1955; Severn 1972). Thus, it is
298 conceivable that teleosts, amphibians, birds and mammalian fetuses have a common architecture
299 in terms of hepatocyte configuration.

300 Second, the position of hepatic artery in the lobule may be different between mammals
301 and zebrafish (Fig. 8). In the former, the hepatic artery is present around portal veins or bile ducts
302 at the periphery of the lobule, and supplies the arterial blood to sinusoids. Thus, the arterial blood
303 may be efficiently supplied to all hepatocytes within the hepatic lobule through sinusoids. However,

304 in the latter, the hepatic artery was located midway between sinusoids (around bile ducts) and along
305 portal veins. Thus, substances from the arterial blood, including oxygen and hormones, may form
306 a more complex pattern in the lobule of the zebrafish than that in mammals.

307 Third, zonation was not found in the liver lobule of zebrafish (Fig. 8). Genes for cell
308 adhesion molecules, metabolic pathways, and the detoxification-related reactions examined, all of
309 which show zonation in mammalian livers, were expressed throughout the hepatic lobule.
310 Furthermore, there was no difference between endothelial cells of portal veins and central veins
311 in expression of genes that are expressed only in portal endothelial cells in mammalian livers.
312 These data indicated that the zebrafish might have acquired a novel functional liver unit from the
313 ancestral one with the portal triad. It has been reported that, in some fishes, multiple genes with
314 normally uniform expression patterns show zonation after treatment such as fasting or liver
315 resection (Schär et al. 1985; Wolf and Wolfe 2005; Olsvik et al. 2007; Zheng et al. 2016). Thus,
316 hepatic zonation can also be formed in the zebrafish liver under stress conditions. More data are
317 required to clarify this issue, including those of gene expression of the Wnt/β-catenin pathway,
318 which plays a key role in hepatic zonation of the mouse (Benhamouche et al. 2006). Although
319 hepatic zonation is detectable in livers of various mammals, but not in those of some birds and
320 amphibians (Smith and Campbell 1988; Wagenaar et al. 1994; Ohno et al. 2008), it is not known
321 whether other tetrapods or primitive vertebrates (e.g., chondrichthyes and hagfish) have hepatic
322 zonation as well. It would be intriguing to analyze the evolutionary trend of hepatic zonation, and
323 clarify when and how mammalian hepatic zonation was established with that of the
324 actinopterygians during vertebrate evolution.

Fourth, the composition of portal blood might be different depending on lobules in the zebrafish (Fig. 8). In the zebrafish, blood was supplied to the liver separately from different segments of the small intestine, which might lead to distinct metabolic loads from lobule to lobule. In contrast, in mammals, mesenteric veins enter the liver after being integrated into a single portal vein, so that each hepatic lobule receives blood with the same composition. In fetal and neonatal mammals, differential hepatic gene expression between the left and right lobes has been demonstrated (Gruenwald 1949; Zhang and Byrne 2000; Cox et al. 2006), which is probably derived from the differential blood supply of the umbilical vein having high oxygenation to the left lobe. Although the gene expression patterns for liver functions examined in this study did not show zonation in the entire liver, detailed analyses of gene expression possibly detect lobar differences or zonation in the zebrafish liver. In the future, elucidation of the biological role of the unique configuration of portal veins in the zebrafish liver will be important to reveal the morphological evolution of actinopterygian livers.

2. Gene expression in the biliary tract system of zebrafish

The present study demonstrated that the biliary tract system of zebrafish had different gene expression patterns depending on the parts according to ISH analyses (Fig. 7). In mice, Pdx1-positive extrahepatic bile ducts can be distinguished from Pdx1-negative intrahepatic bile ducts (Sumazaki et al., 2004; Igarashi et al., 2012). This was also the case in the zebrafish biliary system. In addition, zebrafish orthologs of Hnf1b, important for the development of intrahepatic bile ducts in mammals, and orthologs of Slc4a2b, important for the barrier mechanism of bile ducts, were

346 expressed in both extrahepatic and intrahepatic bile ducts, but not in preductules/ductules. These
347 data indicated that there was a significant difference in gene expression between intrahepatic bile
348 ducts and preductules/ductules in the zebrafish, suggesting that their properties or functions may
349 be different. On the other hand, the present study confirmed expression of *cdh1* and *epcam* in the
350 entire biliary tract system, including preductules/ductules, in addition to *anxa4*, which can detect
351 preductules/ductules in the zebrafish liver (Zhang et al., 2014). Gene expression of *pdx1*, *hnf1b*,
352 *slc4a2b*, *anxa4*, *cdh1* and *epcam* will be useful for analyzing biliary tract development of the
353 zebrafish liver in the future.
354
355 3. Use of the zebrafish as an alternative model for human disease
356 The zebrafish has become an important vertebrate model for embryonic development,
357 toxicity, drug screening and human diseases (Lorent et al. 2004; Matthews et al. 2004; Cui et al.
358 2013). The gene expression patterns in liver lobules and each segment of the bile duct system, and
359 our liver lobule model of the zebrafish may be important to discuss data obtained in experiments
360 using this animal as an alternative model for such purposes. Oval or liver progenitor cell reaction,
361 which may be postulated for ductule cell activation, might occur in a different way in zebrafish
362 livers from in mammal livers. The presence or absence of hepatic zonation in human and zebrafish
363 livers might generate their different responses to various carcinogens or drugs.
364
365 Acknowledgements
366 We thank Professor Emeritus Takeo Mizuno of the University of Tokyo and Prof. Nelson

Fausto of the University of Washington for their continued interest in our study and encouragement, and Mr. Kim Barrymore for his help in preparing our manuscript. The authors also thank Dr. T. Koike and Mr. T. Fukuchi for their discussion and technical support.

Declarations

Funding information

This work was supported in part by a Grant-in-Aid from the Japan Society for the Promotion of Science (JSPS) Fellows from the JSPS (KAKEN Grant Number 18J21880 to N. O.), and a Sasakawa Scientific Research Grant from The Japan Science Society (Research Number 28-447 to N. O.).

Conflict of interest

The authors have no conflicts of interest concerning this article.

Ethical approval

All animal studies have been approved by the Institutional Animal Care and Use Committee for Shizuoka University (approval number: 29F-6, 2018F-8, 2019F-8 and 2020F-9) and have been performed in accordance with the institutional guidelines.

Informed consent

Not applicable.

Author contributions

N. O. and N. S. conceived the study. N. O. carried out all data collection and analysis and wrote the entire manuscript and figures. N. S. provided guidance for data interpretation and manuscript writing and editing. All authors reviewed and approved the final manuscript.

408 References

409

410 Akai Y, Oitate T, Koike T, Shiojiri N (2014) Impaired hepatocyte maturation, abnormal
411 expression of biliary transcription factors and liver fibrosis in C/EBPα (Cebpa)-knockout
412 mice. Histol Histopathol 29:107-125

413 Bartels H, Linnemann H, Jungermann K (1989) Predominant localization of
414 phosphoenolpyruvate carboxykinase mRNA in the periportal zone of rat liver parenchyma
415 demonstrated by in situ hybridization. FEBS Lett 248:188-194

416 Benhamouche S, Decaens T, Godard C, Chambrey R, Rickman DS, Moinard C, Vasseur-Cognet
417 M, Kuo CJ, Kahn A, Perret C, Colnot S (2006) Apc tumor suppressor gene is the "zonation-
418 keeper" of mouse liver. Dev Cell 10:759-770

419 Cox LA, Schlabritz-Loutsevitch N, Hubbard GB, Nijland MJ, Thomas J. McDonald TJ,
420 Nathanielsz PW (2006) Gene expression profile differences in left and right liver lobes from
421 mid-gestation fetal baboons: a cautionary tale. J Physiol 572:59-66

422 Cui S, Leyva-Vega M, Tsai EA, EauClaire SF, Glessner JT, Hakonarson H, Devoto M, Haber
423 BA, Spinner NB, Matthews RP (2013) Evidence from human and zebrafish that GPC1 is a
424 biliary atresia susceptibility gene. Gastroenterology 144:1107-1115

425 Doi Y, Tamura S, Nammo T, Fukui K, Kiso S, Nagafuchi A (2007) Development of
426 complementary expression patterns of E- and N-cadherin in the mouse liver. Hepatol Res
427 37:230-237

428 Elias H (1955) Origin and early development of the liver in various vertebrates. Acta Hepatol 3:1-

56

Faccioli CK, Chedid RA, Bombonato MTS, Vicentini CA, Vicentini IBF (2014) Morphology and histochemistry of the liver of carnivorous fish *Hemisorubim platyrhynchos*. Int J Morphol 32:715-720

Gerbal-Chaloin S, Dumé AS, Briolotti P, Klieber S, Raulet E, Duret C, Fabre JM, Ramos J, Maurel P, Daujat-Chavanieu M (2014) The WNT/b-catenin pathway is a transcriptional regulator of CYP2E1, CYP1A2, and aryl hydrocarbon receptor gene expression in primary human hepatocytes. Mol Pharmacol 86:624-634

Ghafoory S, Breitkopf-Heinlein K, Li Q, Scholl C, Dooley S, Wölfl S (2013) Zonation of nitrogen and glucose metabolism gene expression upon acute liver damage in mouse. PLoS ONE 8:e78262

Gruenwald P (1949) Degenerative changes in the right half of the liver resulting from intra-uterine anoxia. Am J Clin Pathol 19:801-813

Hampton JA, Lantz RC, Goldblatt PJ, Lauren DJ, Hinton DE (1988) Functional units in rainbow trout (*Salmo gairdneri*, Richardson) liver: II. The biliary system. Anat Rec 221:619-634

Hardman RC, Volz DC, Kullman SW, Hinton DE (2007) An in vivo look at vertebrate liver architecture: three-dimensional reconstructions from medaka (*Oryzias latipes*). Anat Rec 290:770-782

448 Hempel M, Schmitz A, Winkler S, Kucukoglu O, Brückner S, Niessen C, Christ B (2015)
449 Pathological implications of cadherin zonation in mouse liver. Cell Mol Life Sci 72:2599-
450 2612
451 Jones EA, Clement-Jones M, Wilson DI (2000) JAGGED 1 expression in human embryos:
452 correlation with the Alagille syndrome phenotype. J Med Genet 37:658-662
453 Jungermann K, Thurman RG (1992) Hepatocyte heterogeneity in the metabolism of
454 carbohydrates. Enzyme 46:33-58
455 Kamimoto K, Nakano Y, Kaneko K, Miyajima A, Itoh T (2020) Multidimensional imaging of
456 liver injury repair in mice reveals fundamental role of the ductular reaction. Commun Biol
457 3:289
458 Kuo FC, Hwu WL, Valle D, Darnell JE Jr (1991) Colocalization in pericentral hepatocytes in
459 adult mice and similarity in developmental expression pattern of ornithine aminotransferase
460 and glutamine synthetase mRNA. Proc Natl Acad Sci USA 88:9468-9472
461 Lorent K, Yeo SY, Oda T, Chandrasekharappa S, Chitnis A, Matthews RP, Pack M (2004)
462 Inhibition of Jagged-mediated notch signaling disrupts zebrafish biliary development and
463 generates multi-organ defects compatible with an Alagille syndrome phenocopy.
464 Development 131:5753-5766
465 Lu JW, Ho YJ, Yang YJ, Liao HA, Ciou SC, Lin LI, Ou DL (2015) Zebrafish as a disease model
466 for studying human hepatocellular carcinoma. World J Gastroenterol 21:12042-12058

467 Matthews RP, Lorent K, Russo P, Pack M (2004) The zebrafish onecut gene hnf-6 functions in an
468 evolutionarily conserved genetic pathway that regulates vertebrate biliary development. Dev
469 Biol 274:245-259
470 Moorman AF, de Boer PA, Geerts WJ, van den Zande L, Lamers WH, Charles R (1988)
471 Complementary distribution of carbamoylphosphate synthetase (ammonia) and glutamine
472 synthetase in rat liver acinus is regulated at a pretranslational level. J Histochem Cytochem
473 36:751-755
474 Igarashi S, Matsubara T, Harada K, Ikeda H, Sato Y, Sasaki M, Matsui O, Nakanuma Y (2012)
475 Bile duct expression of pancreatic and duodenal homeobox 1 in perihilar
476 cholangiocarcinogenesis. Histopathology 61:266-276
477 Ohno H, Naito Y, Nakajima H, Tomita M (2008) Construction of a biological tissue model based
478 on a single-cell model: a computer simulation of metabolic heterogeneity in the liver lobule.
479 Artif Life 14:3-28
480 Olsvik PA, Lie KK, Saele Ø, Sanden M (2007) Spatial transcription of CYP1A in fish liver.
481 BMC Physiol 7:12
482 Ota N, Hirose H, Kato H, Maeda H, Shiojiri N (2021) Immunohistological analysis on distribution
483 of smooth muscle tissues in livers of various vertebrates with attention to different liver
484 architectures. Ann Anat 233:151594
485 Petcoff GM, Díaz AO, Escalante AH, Goldemberg AL (2006) Histology of the liver of
486 *Oligosarcus jenynsii* (Ostariophysi, Characidae) from Los Padres Lake, Argentina. Iheringia
487 Sér Zool 96:205-208

488 Rocha E, Monteiro RAF, Pereira CA (1995) Microanatomical organization of hepatic stroma of
489 the brown trout, *Salmo trutta fario* (Teleostei, Salmonidae): a qualitative and quantitative
490 approach. J Morphol 223:1-11
491 Schindelin J, Arganda-Carreras I, Frise E, Kaynig V, Longair M, Pietzsch T, Preibisch S, Rueden
492 C, Saalfeld S, Schmid B, Tinevez JY, White DJ, Hartenstein V, Eliceiri K, Tomancak P,
493 Cardona A (2012) Fiji: an open-source platform for biological-image analysis. Nat Methods
494 9:676-682
495 Schär M, Maly IP, Sasse D (1985) Histochemical studies on metabolic zonation of the liver in the
496 trout (*Salmo gairdneri*). Histochemistry 83:147-151
497 Schmid B, Schindelin J, Cardona A, Longair M, Heisenberg M (2010) A high-level 3D
498 visualization API for Java and ImageJ. BMC Bioinformatics 11:274
499 Severn C B (1972) A morphological study of the development of the human liver. II.
500 Establishment of liver parenchyma, extrahepatic ducts and associated venous channels. Am J
501 Anat 133:85-107
502 Shiojiri N, Kametani H, Ota N, Akai Y, Fukuchi T, Abo T, Tanaka S, Sekiguchi J, Matsubara S,
503 Kawakami H (2018) Phylogenetic analyses of the hepatic architecture in vertebrates. J Anat
504 232:200-213
505 Shiojiri N, Niwa T, Sugiyama Y, Koike T (2006) Preferential expression of connexin37 and
506 connecxin40 in the endothelium of the portal veins during mouse liver development. Cell
507 Tissue Res 324:547-552

508 Sumazaki R, Shiojiri N, Isoyama S, Masu M, Keino-Masu K, Osawa M, Nakauchi H, Kageyama
509 R, Matsui A (2004) Conversion of biliary system to pancreatic tissue in Hes1-deficient mice.
510 Nat Genet 36:83-87
511 Smith DD, Campbell JW (1988) Distribution of glutamine synthetase and carbamoyl-phosphate
512 synthetase I in vertebrate liver. Proc Natl Acad Sci USA 85:160-164
513 Umezu A, Kametani A, Akai Y, Koike T, Shiojiri N (2012) Histochemical analyses of hepatic
514 architecture of the hagfish with special attention to periportal biliary structures. Zool Sci
515 29:450-457
516 Wagenaar GT, Moorman AF, Chamuleau RA, Deutz NE, De Gier C, De Boer PA, Verbeek FJ,
517 Lamers WH (1994) Vascular branching pattern and zonation of gene expression in the
518 mammalian liver. A comparative study in rat, mouse, cynomolgus monkey, and pig. Anat
519 Rec 239:441-452
520 Wolf JC, Wolfe MJ (2005) A brief overview of nonneoplastic hepatic toxicity in fish. Toxicol
521 Pathol 33:75-85
522 Yao Y, Lin J, Yang P, Chen Q, Chu X, Gao C, Hu J (2012) Fine structure, enzyme
523 histochemistry, and immunohistochemistry of liver in zebrafish. Anat Rec 295:567-576
524 Yu H, Yoo PK, Aguirre CC, Tsoa RW, Kern RM, Grody WW, Cederbaum SD, Iyer RK (2003)
525 Widespread expression of arginase I in mouse tissues: biochemical and physiological
526 implications. J Histochem Cytochem 51:1151-1160

527 Zhang D, Golubkov VS, Han W, Correa RG, Zhou Y, Lee S, Strongin AY, Dong PD (2014)
528 Identification of Annexin A4 as a hepatopancreas factor involved in liver cell survival. Dev
529 Biol 395:96-110
530 Zhang J, Byrne CD (2000) Differential hepatic lobar gene expression in offspring exposed to
531 altered maternal dietary protein intake. Am J Physiol Gastrointest Liver Physiol 278:G128-
532 G136
533 Zheng JL, Zhu QL, Shen B, Zeng L, Zhu AY, Wu CW (2016) Effects of starvation on lipid
534 accumulation and antioxidant response in the right and left lobes of liver in large yellow
535 croaker *Pseudosciaena crocea*. Ecol Indic 66:269-274
536
537
538
539

Supplementary materials:

Legends for Supplementary Tables

Supplementary Table 1. Primary antibodies used in immunohistochemistry

Supplementary Table 2. Secondary antibodies used in immunohistochemistry

Supplementary Table 3. Primers used in RT-PCR analysis

Supplementary Table 4. Probes used in *in situ* hybridization analysis

Supplementary Table 5. Expression of various mammalian hepatic marker genes in the zebrafish liver

Legends for Supplementary Figures

Supplementary Fig. 1 Anatomy and morphology of the zebrafish liver. a, Left thoraco-laparotomy of the zebrafish. b, Internal organs dissected out. c, H-E staining of serial sections of internal organs. The liver is around the intestine, which is folded twice in the body cavity (a, c). Although it consists of three lobes, they fuse in the anterior part (b). The pancreas resides between the intestine and liver with no definite shape (c). He, heart; In, intestine; Li, liver; Ov, ovary; Pa, pancreas

Supplementary Fig. 2 Blood vessels in the pancreas connect with hepatic sinusoids. a, b, ALP staining of near sections. c, ALP staining in serial sections at intervals of 10 μm. Portal veins often enter the liver with accompanying pancreatic tissue around them (yellow area in a' and b')(a, b). The pancreatic tissue has ALP-positive blood vessels (arrowheads), which connect with hepatic sinusoids (c). Areas surrounded by red lines indicate portal veins. Pa, pancreas; PV, portal vein

Supplementary Fig. 3 Distribution of the hepatic artery in the zebrafish liver. a-d, ALP staining in serial sections. In the liver, the ALP-positive hepatic artery (red arrowhead) resides around intrahepatic bile ducts (a, b). In the extrahepatic area, the hepatic artery is located around the extrahepatic bile duct, and enters the liver with the bile duct (c, d). Yellow dotted line indicates the border between the inside and outside of the liver. BD, bile duct; CV, central vein; EHBD, extrahepatic bile duct

Supplementary Fig. 4 Blood vessel from gonads enters the central vein of the zebrafish liver. a, image under dissection microscope. b-e, ALP staining. Blood vessels (arrowheads) from the ovary enter the liver (surrounded by green dotted line)(a). ALP-negative blood vessels (orange ellipse) merge with the central vein of the liver in serial sections at intervals of 30 μm (b-e). Red frame area of b corresponds to c. CV, central vein; In, intestine; Li, liver; Ov, ovary

Supplementary Fig. 5 Penetration of cholangiocytes of preductules into the canalicular region of hepatocytes in the zebrafish liver. a, H-E staining. b, anxa4 immunohistochemistry poststained with

hematoxylin. Cholangiocytes of preductules (white and black arrows) penetrate into the bile canalicular region of hepatocytes (a, b). BD, bile duct; V, vein

Supplementary Fig. 6 Gene expression analysis of orthologs of mammalian zonation markers in the zebrafish liver with ISH. a-d, *arg2*, *oat*, *pck1* and *glulb* expression, respectively. Although *Arg*, *Oat*, *Pepck1 and Glul* are known to be genes showing expression patterns of zonation in the mouse liver, their orthologs *arg2*, *oat*, *pck1* and *glulb* have uniform expression patterns in hepatocytes of the zebrafish (a-d). CV, central vein; PV, portal vein

Supplementary Fig. 7 Control experiments of ISH for *cdh1* and *cdh2* expression in the small intestine, pancreas and liver of the zebrafish. a, d, antisense probes for *cdh1* and *cdh2*, respectively. b, c, sense probes for *cdh1*. e, f, sense probes for *cdh2*. *cdh1* is specifically expressed in the intestinal mucosal epithelium (a). Antisense probe of *cdh2* reacts with cells of the islet of Langerhans (d). Sense probes of *cdh1* and *cdh2* give negative or very weak signals in the intestine (b), islet of Langerhans (e) and liver (c, f). Red arrowheads indicate the islet of Langerhans. V, vein

Supplementary Fig. 8 Gene expression analysis of orthologs of mammalian portal vein markers in the zebrafish liver with ISH. a-d, *gja5a*, *gja5b*, *jag1a* and *jag1b* expression, respectively. Although expression of Gja5 and Jag1 is detected in endothelial cells of portal veins in the mouse liver, that of their orthologs *gja5a*, *gja5b*, *jag1a* and *jag1b* was not restricted to portal veins (a-d). BD, bile duct; CV, central vein; PV, portal vein

602

603

604 Legend for Supplementary movies

605

606 **Supplementary movies 1 and 2** Movies for three-dimensional reconstruction of sinusoidal ALP
607 staining shown in Fig. 3 at low (10 sections) and high (13 sections) magnification, respectively.
608 Portal veins, central veins and intrahepatic bile ducts are indicated as filled red, blue and green
609 areas, respectively

610

611

612

613

614

615

616

617

618

619

620

621

622

623 Legends for Figures

624

625 **Fig. 1** Entry of the extrahepatic bile duct into the liver of the zebrafish. a-i, H-E staining of serial
626 sections of the extrahepatic bile duct at every 30 μm. Although only one extrahepatic bile duct
627 connects the liver with the intestine, it does not merge with the main pancreatic duct, which enters
628 the intestinal tract independently (a). Branches of the extrahepatic bile duct enter the liver at
629 multiple sites (arrowheads) (a-i). There is no association of the entry of bile ducts with portal
630 veins. EHBD, extrahepatic bile duct; In, intestine; Li, liver; MPD, main pancreatic duct; Pa,
631 pancreas; PV, portal vein

632

633 **Fig. 2** Visualization of sinusoidal orientation in the zebrafish liver by ALP activity staining. a, ALP
634 staining. b, b', ALP staining and its binary processing image with Image, respectively. Three
635 branches of portal veins enter the liver at different locations (a', a'', and a''' in a). Typical portal
636 veins in adjoining sections of a, which enter the liver from the locations a', a'' and a''', are shown
637 at a higher magnification. Sinusoids run between the portal vein and central vein (b). A thick red
638 line indicates a sinusoid connecting the portal vein and central vein (b'). In a and b, some portal
639 and central veins are surrounded by red and blue lines, respectively. CV, central vein; In,
640 intestine; Li, Liver; Pa, pancreas, PV, portal vein

641

642 **Fig. 3** Visualization of liver lobule by three-dimensional reconstruction of sinusoid orientation. a,
643 b, ALP staining. c, three-dimensional reconstruction of sinusoidal ALP staining (10 serial

644 sections). Locations of the portal vein (filled red areas) and central vein (filled blue areas), and
645 orientation of sinusoids in the zebrafish liver are similar to those of mammalian hepatic lobules (a',
646 b'), and have a polygonal leaflet structure indicated by yellow lines and the area in purple (a", a").
647 Intrahepatic bile ducts (filled green areas) are located inside the lobule (a", b"). Three-dimensional
648 reconstruction analysis indicates that spatial sinusoidal orientation is radial from the central vein to
649 peripheral portal veins (c, c'). BD, bile duct; CV, central vein; In, intestine; Ov, ovary; PV, portal
650 vein
651
652 **Fig. 4** Visualization of bile preductule/ductule network by detection of anxa4 expression in the
653 zebrafish liver. a, b, double staining of sinusoidal ALP activity and anxa4 immunohistochemistry.
654 c, c', ISH analyses of *anxa4* expression. anxa4-positive preductules, which penetrate a tubular
655 lumen of hepatocytes, and ductules, are reticulated in the entire lobule unit (a, b). Gene
656 expression of *anxa4* is found in preductules and ductules (c, c'), which is similar to the
657 immunohistochemical detection of anxa4. White and red arrowheads indicate bile ducts and
658 preductules/ductules, respectively. BD, bile duct; V, vein
659
660 **Fig. 5** Zonation in mouse and zebrafish livers. a-g, mouse liver. h-m, zebrafish liver. a, h, PAS
661 staining. b-g, immunohistochemistry of GS, Cyp1a2, Cyp2e1, E-cadherin, and N-cadherin, and
662 double immunostaining of E-cadherin and N-cadherin, respectively. i-m, ISH of *glula*, *cyp1a*,
663 *cyp2y3*, *cdh1* and *cdh2* expression, respectively. Glycogen accumulation is different in periportal
664 and pericentral hepatocytes of the mouse liver, but uniformly observed in hepatocytes of the

zebrafish liver (a, h). Expression of GS, Cyp1a2, and Cyp2e1 is observed in pericentral hepatocytes, but not in periportal hepatocytes of the mouse liver (b-d). Their orthologue mRNAs are uniformly expressed in hepatic lobules of the zebrafish liver (i-k). In the mouse liver, expression of E-cadherin (Cdh1) and N-cadherin (Cdh2) is restricted to periportal and pericentral hepatocytes, respectively (e-g). In contrast, in the zebrafish liver, *cdh1* is not detectable in hepatocytes, but *cdh2* is uniformly expressed in all hepatocytes (l, m). Expression of *cdh1* is found in preductule/ductule cells residing throughout the zebrafish liver (l). CV, central vein; PV, portal vein; V, vein

Fig. 6 Gene expression in the bile duct/ductule system of zebrafish analyzed with ISH. a-c, *cdh1* expression. d-f, *epcam* expression. g-i, *hnf1ba* expression. j-l, *slc4a2b* expression. m-o, *pdx1* expression. Expression of *cdh1* and *epcam* is confirmed in all epithelial cells of extrahepatic bile ducts, intrahepatic bile ducts and preductules/ductules, similarly to anxa4 expression (a-f). On the other hand, gene expression of *hnf1ba* and *slc4a2b* and is detected in epithelial cells of extra- and intrahepatic bile ducts, but not in preductules/ductules (g-l). Expression of *pdx1* is confirmed only in epithelial cells of the extrahepatic bile duct (m-o). Extrahepatic bile ducts, intrahepatic bile ducts and preductules/ductules are indicated by green arrowheads, red circles and red arrowheads, respectively. EHBD, extrahepatic bile duct; IHBD, intrahepatic bile duct

Fig. 7 Comparison of gene expression in the biliary systems of the mouse and zebrafish. In the mouse, intrahepatic bile duct cells basically share marker genes with ductule cells. However, in the zebrafish, some markers such as bile duct-specific cytokeratin, *hnf1ba* and *hnf1bb* are expressed in

686 intrahepatic bile duct cells, but not in preductule/ductule cells. In both the mouse and zebrafish,
687 Pdx1 is expressed in extrahepatic bile ducts. Intrahepatic bile ducts and preductules/ductules do
688 not express Pdx1. CK, cytokeratin; EHBD, extrahepatic bile duct; IHBD, intrahepatic bile duct
689
690 **Fig. 8** Unit structures of the mouse and zebrafish livers. Both mouse and zebrafish livers are
691 composed of histological units with polygonal structures (polygonal pillars in the mouse).
692 Although the unit in the zebrafish is thought hepatic lobules, it has several traits different from
693 those of the mouse. In the mouse, intrahepatic bile ducts are restricted to periportal areas, whereas
694 in the zebrafish they are randomly distributed in hepatic lobules. The major bile transport across
695 hepatic lobules is performed through bile canaliculi of hepatocytes in the mouse, but through
696 hepatic tubules with preductules in the zebrafish, which form a reticulate network in the liver. The
697 hepatic zonation characteristic of mammalian livers is not confirmed in the zebrafish liver. In the
698 mouse, the portal vein is a single blood vessel, and branches before entering the liver. Multiple
699 portal veins enter the liver independently from the intestine in the zebrafish. CV, central vein; PV,
700 portal vein
701

Fig. 1

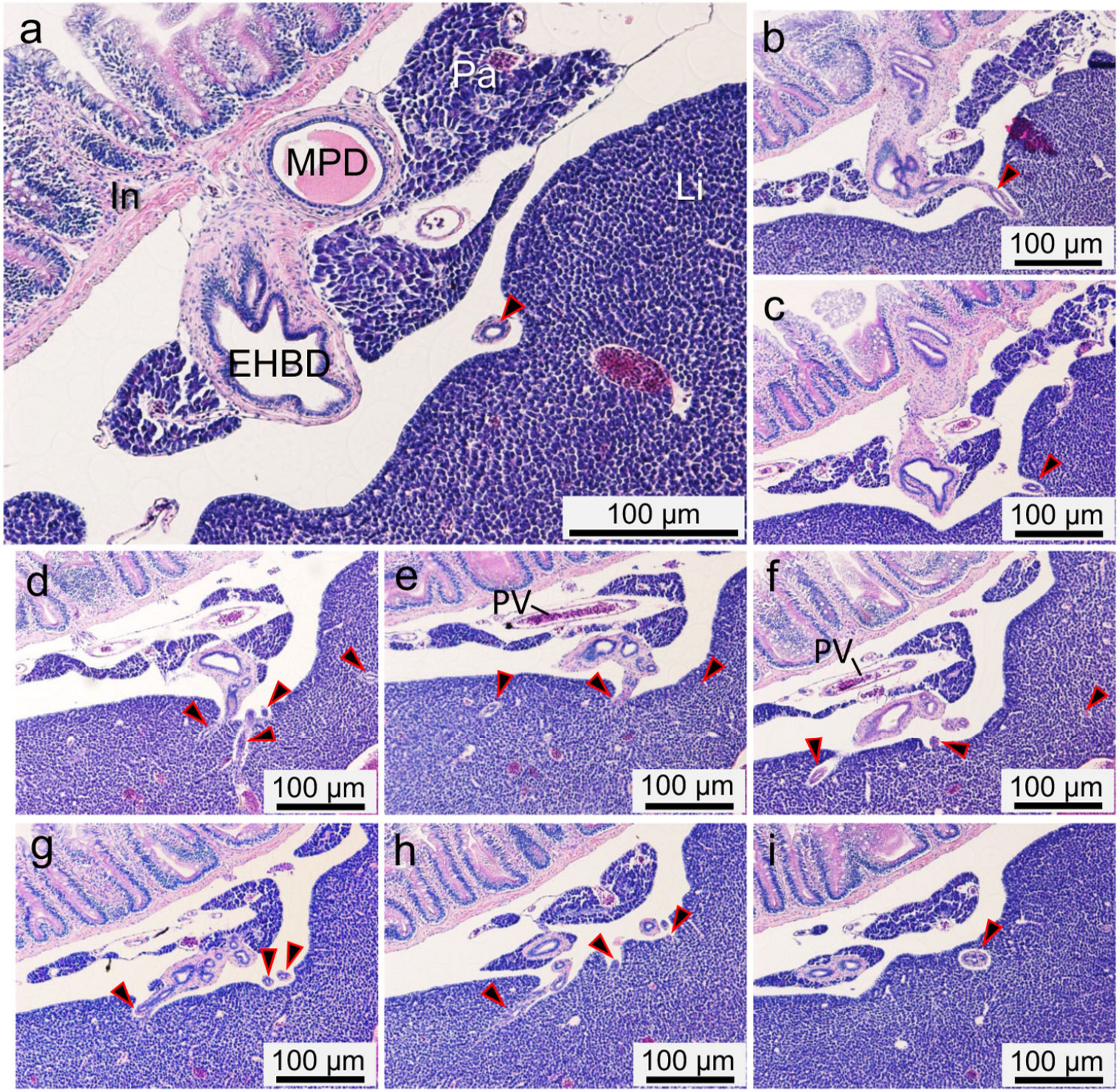
a
Pa
MPD
In
Li
EHBD
100 μm
b
100 μm
c
100 μm
d
100 μm
e
PV
100 μm
f
PV
100 μm
g
100 μm
h
100 μm
i
100 μm

Fig. 2

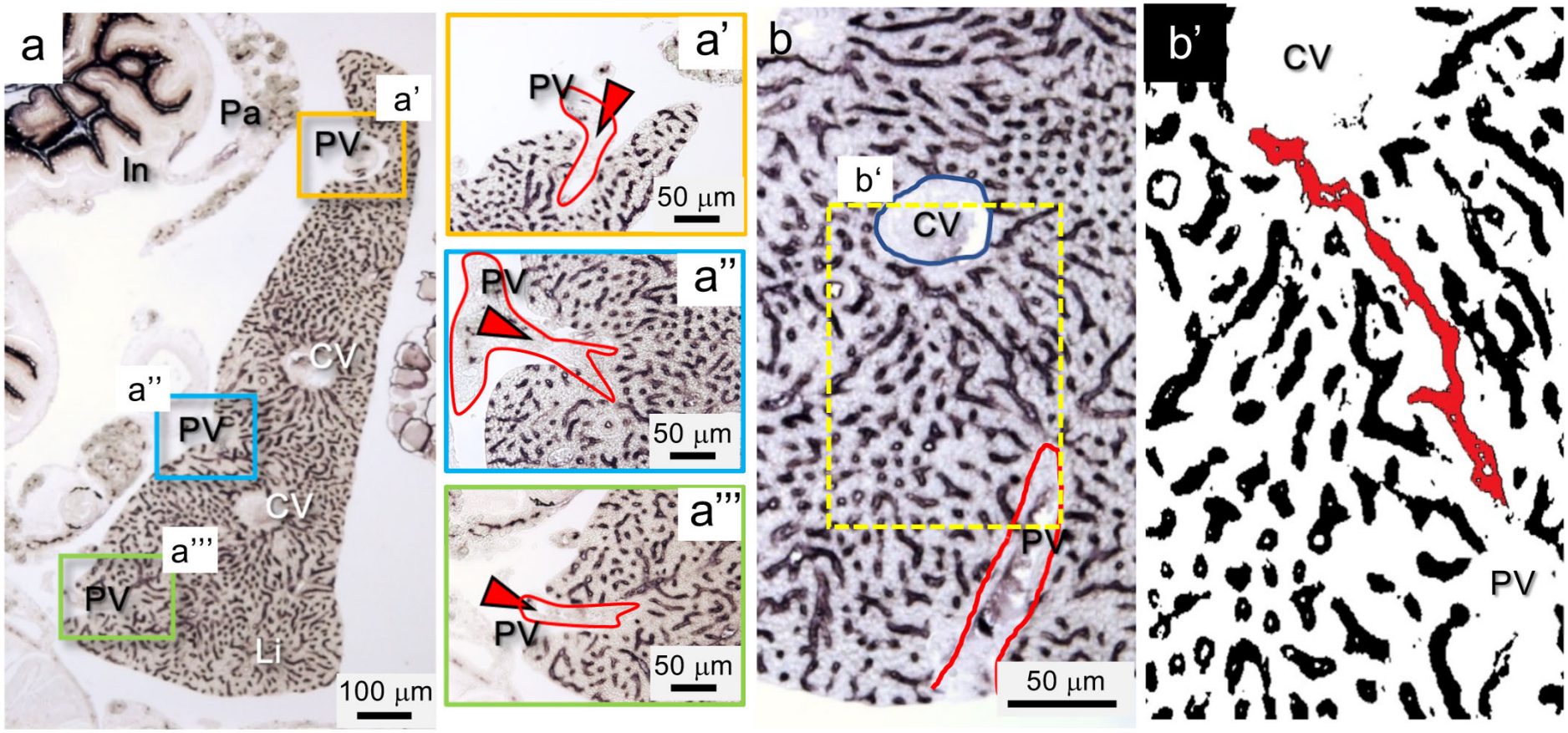
a
Pa
In
a'
PV
CV
a''
PV
CV
a'''
PV
Li
100 µm
a'
PV
50 µm
a''
PV
50 µm
a'''
PV
50 µm
b
b'
CV
PV
50 µm
b'
CV
PV

Fig. 3

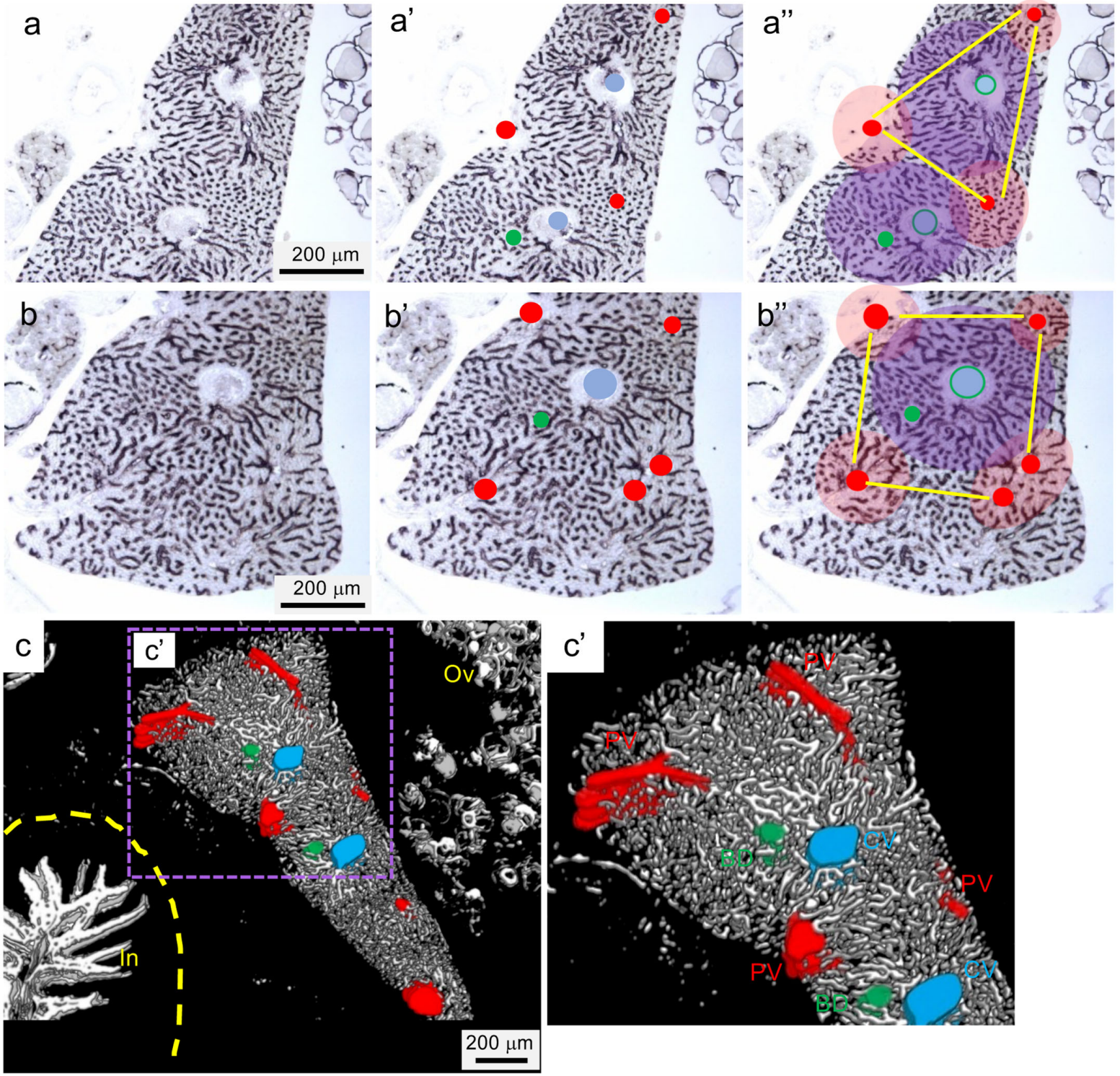

Fig. 4

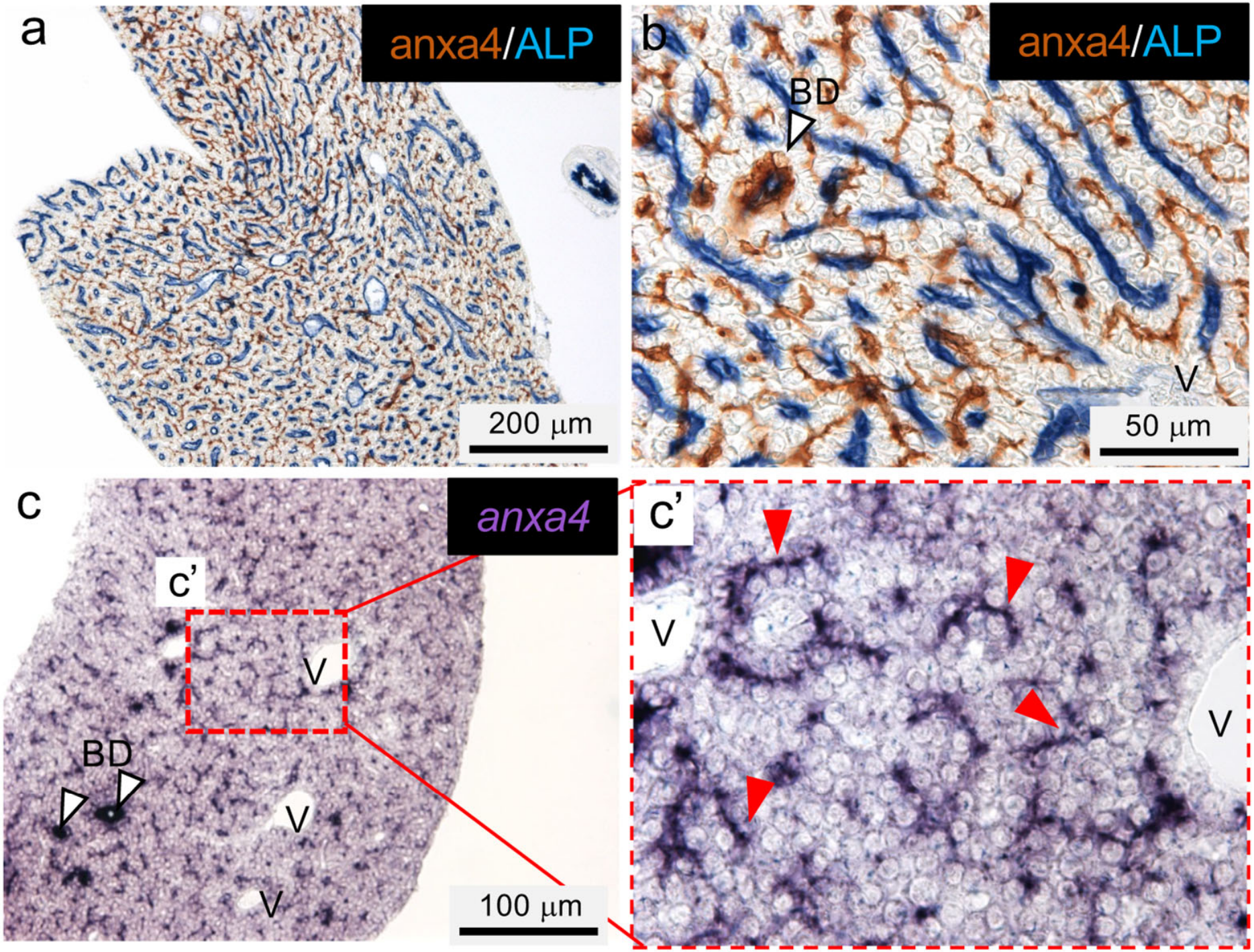
a
anxa4/ALP
200 μm
b
anxa4/ALP
BD
V
50 μm
c
anxa4
c'
V
BD
V
V
100 μm
c'
V
V

Fig. 5

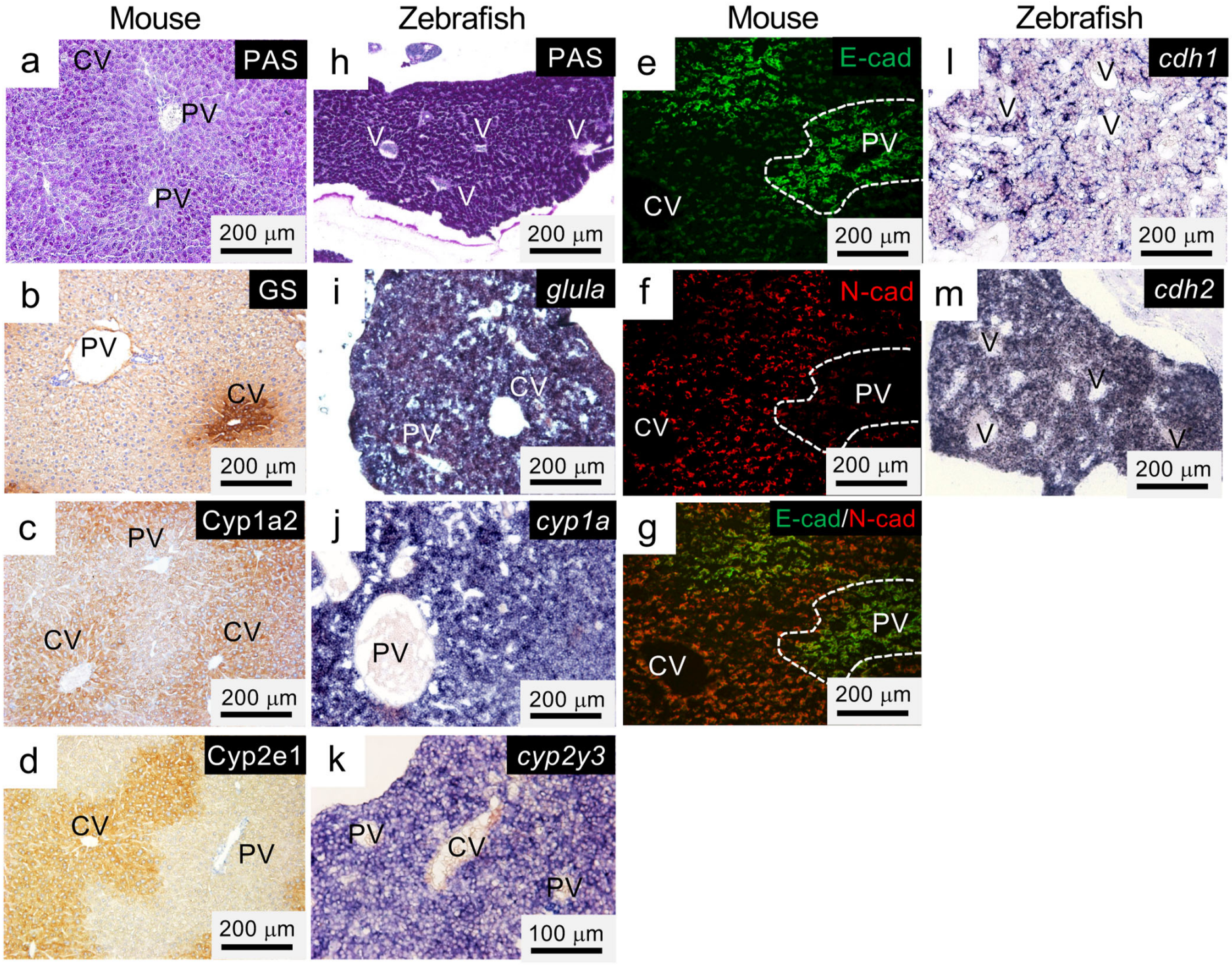
Mouse
Zebrafish
Mouse
Zebrafish
a
CV
PAS
PV
PV
200 μm
h
PAS
V
V
V
V
200 μm
e
E-cad
PV
CV
200 μm
l
cdh1
V
V
V
200 μm
b
GS
PV
CV
200 μm
i
glula
CV
PV
200 μm
f
N-cad
PV
CV
200 μm
m
cdh2
V
V
V
V
200 μm
c
Cyp1a2
PV
CV
CV
200 μm
j
cyp1a
PV
200 μm
g
E-cad/N-cad
PV
CV
200 μm
d
Cyp2e1
CV
PV
200 μm
k
cyp2y3
PV
CV
PV
100 μm

Fig. 6

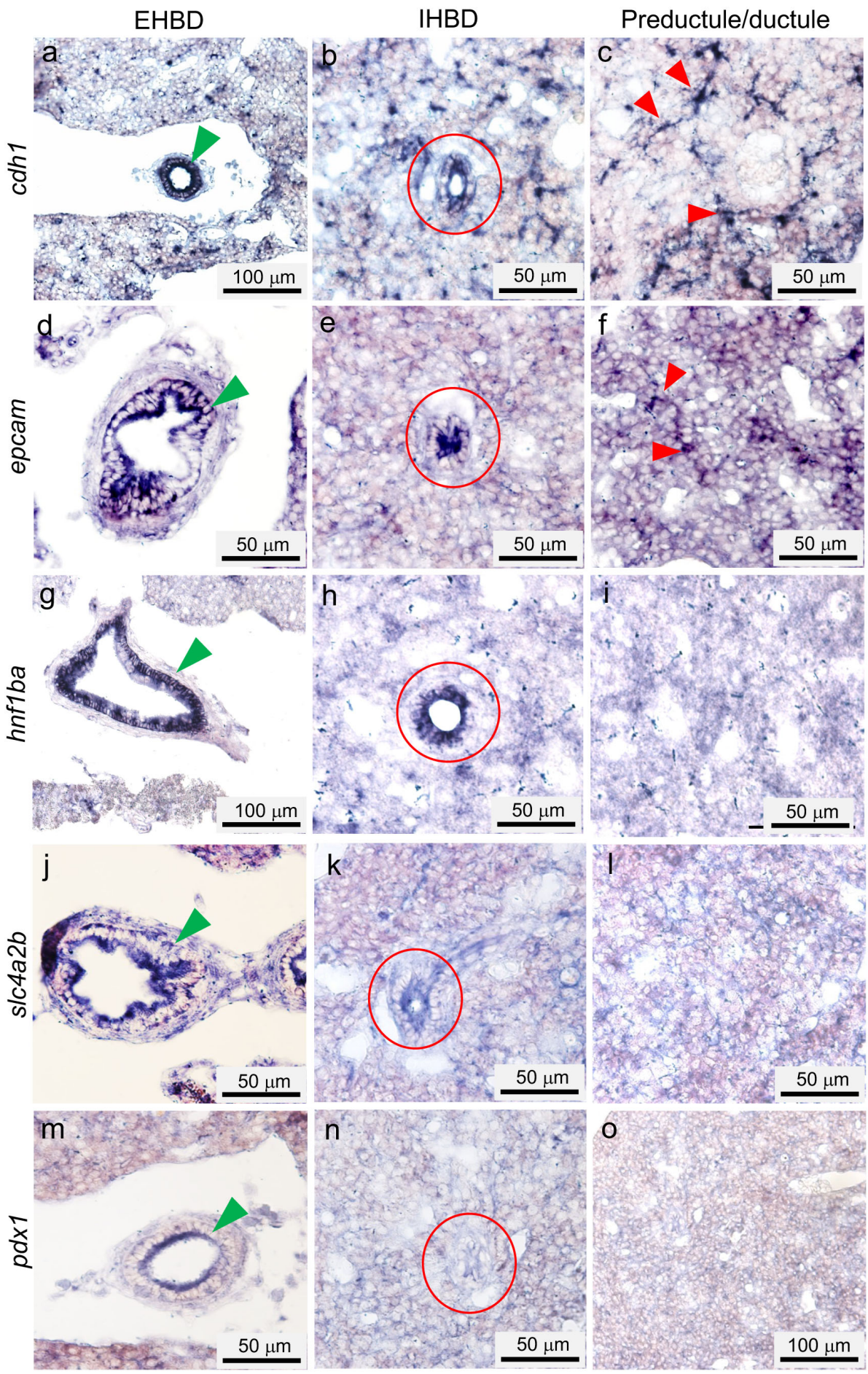
EHBD
IHBD
Preductule/ductule
cdh1
epcam
hnf1ba
slc4a2b
pdx1
a
b
c
d
e
f
g
h
i
j
k
l
m
n
o
100 µm
50 µm
50 µm
50 µm
50 µm
100 µm
50 µm
50 µm
50 µm
50 µm
50 µm
50 µm
100 µm

Fig. 7

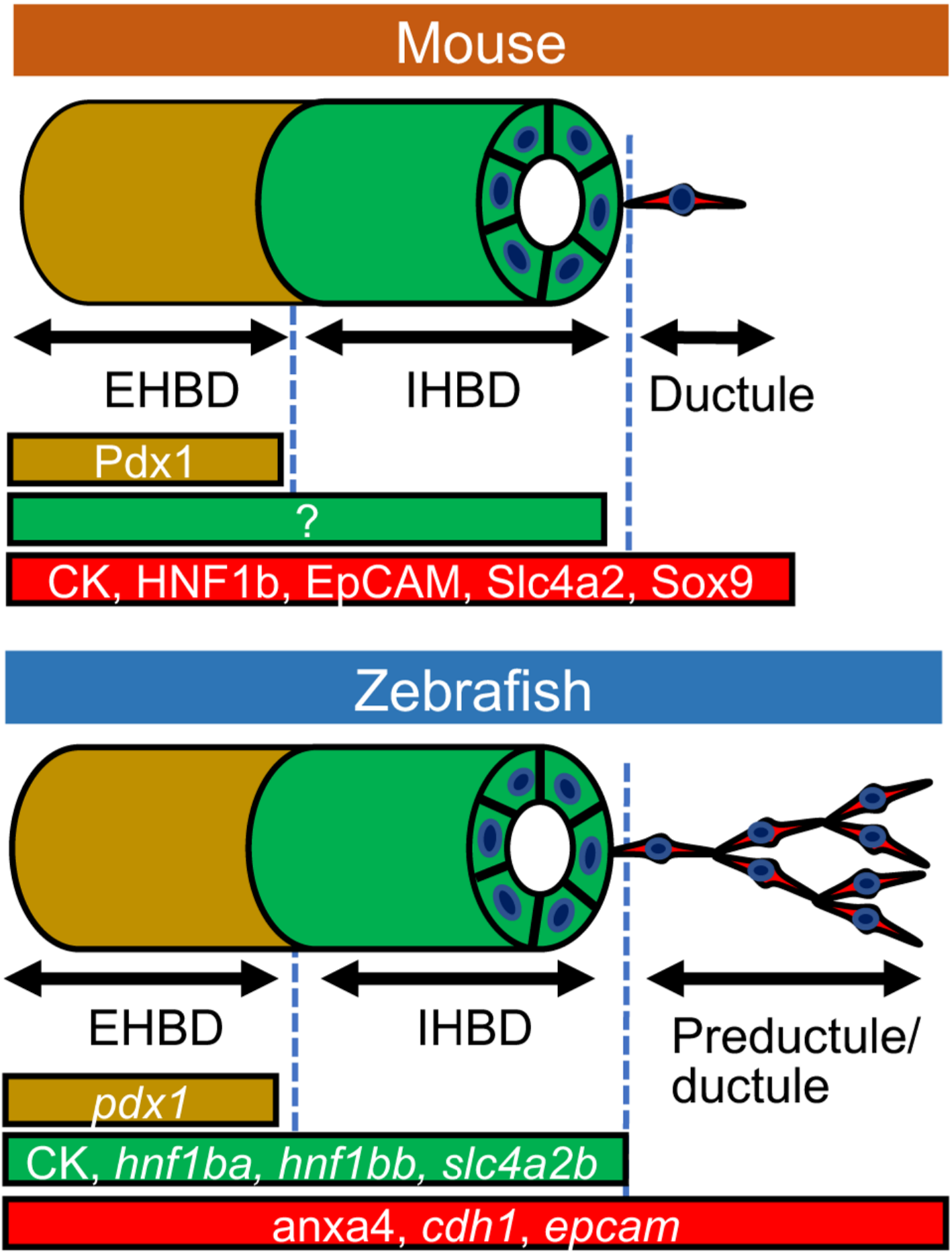
Mouse
EHBD
IHBD
Ductule
Pdx1
?
CK, HNF1b, EpCAM, Slc4a2, Sox9
Zebrafish
EHBD
IHBD
Preductule/
ductule
pdx1
CK, hnf1ba, hnf1bb, slc4a2b
anxa4, cdh1, epcam

Fig. 8

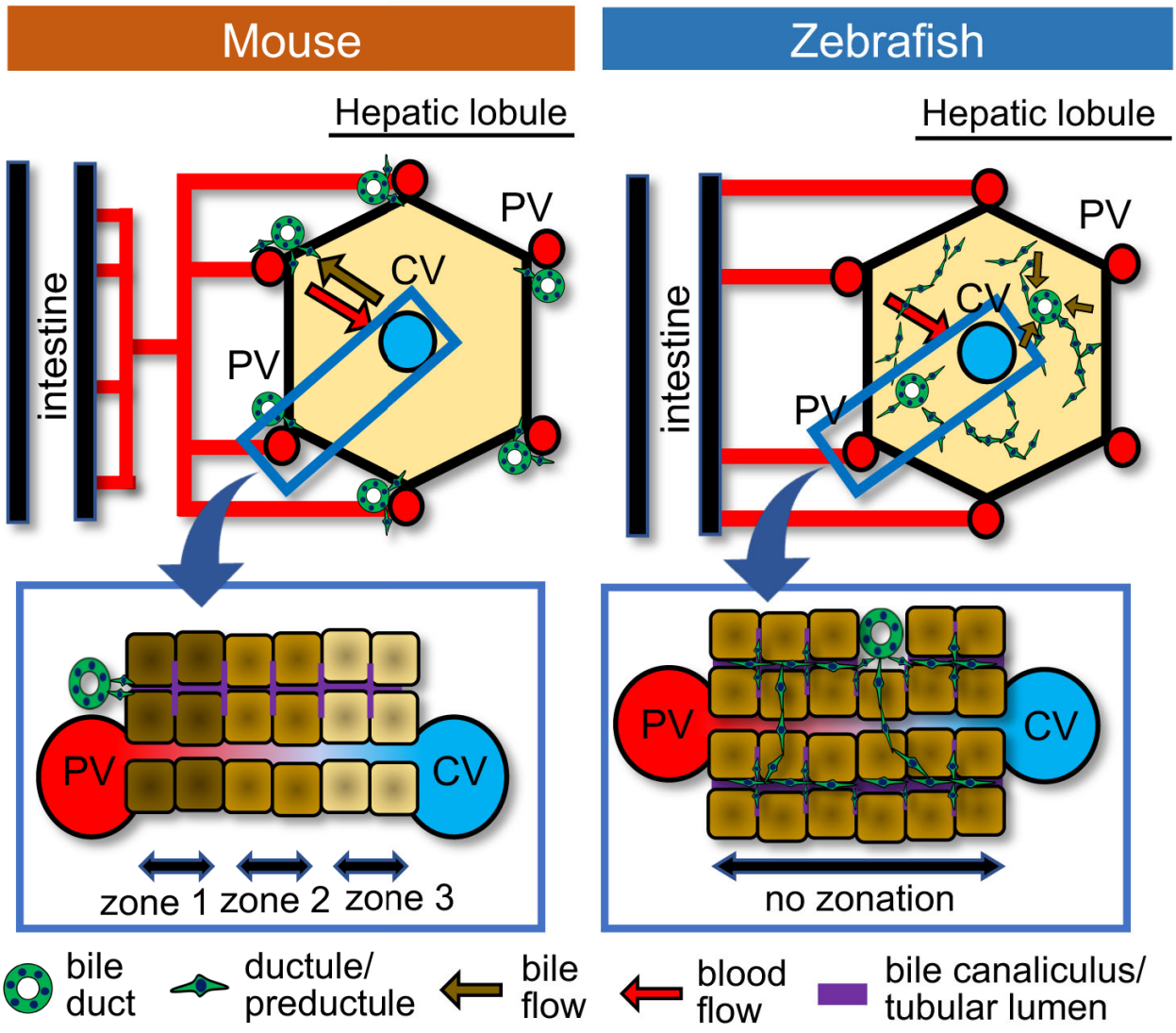

Mouse	Zebrafish
Location of intrahepatic bile ducts	
only periportal	random in the lobule
No. of independent portal vessels entering the liver from the intestine	
single	many
Bile transport cells in the hepatic lobule	
bile canaliculus of hepatocytes	tubules of hepatocytes with preductules
Hepatic zonation	
Yes	No